

## Article

# Influence of Biochar and Modified Polyglutamic Acid Co-Coated Urea on Crop Growth and Nitrogen Budget in Rice Fields

Lei Wei <sup>1,2</sup>, Lin Cheng <sup>1,\*</sup>, Fuxing Guo <sup>2</sup> , Fuyong Wu <sup>2</sup> and Yanping Wang <sup>2</sup>

<sup>1</sup> School of Hydraulic Engineering, Wanjiang University of Technology, Maanshan 243000, China; weilei106@163.com

<sup>2</sup> College of Natural Resources and Environment, Northwest A&F University, Yangling 712100, China; fuxing.guo@nwfau.edu.cn (F.G.); wfy09@163.com (F.W.); ylwangyp@163.com (Y.W.)

\* Correspondence: chenglin0124@163.com; Tel.: +86-0555-5222694

**Abstract:** Natural superabsorbent polymers (SAPs) were essential coating materials for developing slow-release fertilizers (SRFs) due to low cost and biodegradability. However, conventional natural SAPs were unsuitable for rice systems due to low stability and short slow-release period. Herein, a natural SAP with a semi-interpenetrating polymer network was prepared by poly ( $\gamma$ -glutamic acid) (PGlu), diatomite, and pullulan polysaccharide and combined with biochar to develop double-layer co-coated slow-release urea for rice systems. The results indicated that diatomite and pullulan modification significantly improved the slow-release capacity of SAP, with a significant increase in the average fertilizer <sup>15</sup>N content of the soil profile by  $37.9 \pm 7.4\%$  in 14–56 days. The improved slow-release capacity had significant benefits for the sustainability of the rice system, which increased plant N uptake by  $17.2 \pm 4.8\%$ , decreased fertilizer N losses by  $30.4 \pm 7.2\%$ , and increased rice grain yield by  $9.88 \pm 3.6\%$ . More importantly, this natural SAP was fully degradable and its decomposition products are large amounts of small-molecule nutrients that could provide additional C, N, and Si to rice. Therefore, novel co-coated SRF may emerge as a greatly promising candidate for future intensive paddies.

**Keywords:** slow-release fertilizers; superabsorbent polymers; biochar; nitrogen isotope tracing; nitrogen use efficiency; nitrogen losses



**Citation:** Wei, L.; Cheng, L.; Guo, F.; Wu, F.; Wang, Y. Influence of Biochar and Modified Polyglutamic Acid Co-Coated Urea on Crop Growth and Nitrogen Budget in Rice Fields. *Agriculture* **2024**, *14*, 2212. <https://doi.org/10.3390/agriculture14122212>

Received: 23 October 2024

Revised: 26 November 2024

Accepted: 29 November 2024

Published: 3 December 2024



**Copyright:** © 2024 by the authors. Licensee MDPI, Basel, Switzerland. This article is an open access article distributed under the terms and conditions of the Creative Commons Attribution (CC BY) license (<https://creativecommons.org/licenses/by/4.0/>).

## 1. Introduction

Rice cropping systems have been a hotspot for global N losses, which were estimated to emit up to 2 million tons of reactive N into the environment annually [1,2]. Rice requires a proper and constant supply of N during growth [3]. However, synthetic fertilizers have extremely rapid rates of nutrient release and can release a large amount of reactive N in a short period [2,4]. This excess and unstable reactive nitrogen cannot be taken up by the plant root system promptly, thus becoming an essential source of global nitrogen loss through leaching, volatilization, and denitrification [2–5]. Coated slow-release fertilizers (SRFs) promise to reduce nitrogen loss from paddy fields by replacing conventional synthetic fertilizers [4–6]. Through encapsulating a coating on the fertilizer particles, coated SRFs can restrict the nutrient release rate and prolong the fertilization effect, thus reducing field fertilizer loss and input [7–9]. Various hydrophobic inorganic or organic coating materials such as sulfur, paraffin, resins, etc., and their combinations were investigated to improve the N use efficiency [10,11]. However, few of these coating materials and combinations were suitable for large-scale application to rice cropping systems [5,12]. Limited raw materials, high costs, poor water stability, and degradability bring uncertainty to the promotion and application of coated SRFs [13,14]. Therefore, the development of low-cost, renewable, and eco-friendly coating materials has attracted considerable attention.

Organic superabsorbent polymers (SAPs) are potential new favorites for agricultural coating materials due to excellent water and fertilizer retention properties [15–18].

Compared to inorganic coating materials, SAPs were environmentally sensitive (e.g., soil temperature, pH, etc.) and their nutrient release curves were more closely linked to the plant growth requirements [11,19,20]. Current SAPs in studies and commerce are dominated by synthetic SAPs with -C-C-type, such as polyacrylic acid and polyvinyl alcohol [10–12,15,17,21–25]. SAPs with -C-C-type have high molecular weight, structural stability, and water absorption. However, synthetic SAPs are carcinogenic, poorly biodegradable, and may cause environmental risk [11,19]. Moreover, the raw materials for synthetic SAPs are nonrenewable petroleum resources with high processing costs [16]. Natural SAPs mainly include three types, starch-SAPs, cellulose-SAPs, and protein-SAPs, which have great potential for application because they are environmentally friendly, degradable, and nontoxic [18,26]. Raw materials for natural SAPs are mostly agricultural wastes, which are easily renewable and support the United Nations Sustainable Development Goals (SDGs) [16,27]. However, the structure of natural SAPs was unstable and, when they were used as coating materials, the slow-release period was short and required modification and strengthening.

$\gamma$ -polyglutamic acid (PGlu) is a naturally homozygous polyamine produced from L-glutamic acid and D-glutamic acid monomers [20,22,28]. Due to the large number of carboxyl groups on the branched chain, the structure of PGlu is easy to modify to fulfill various demands [21,29]. Thus, PGlu has a wide range of applications covering biomedicine, food, cosmetics, and agriculture [11,21,28,30]. PGlu is fermented by microorganisms, and the raw materials are inexpensive and renewable, mostly agricultural wastes such as soybean dregs and manure [17,31]. PGlu is environmentally benign and can be degraded by microorganisms and enzymes in soil to short peptides or glutamic acid monomers, which ultimately act as nutrient enhancers and provide nitrogen sources for crop growth [16]. Moreover, SAPs produced by PGlu are extremely water-absorbent and could reach thousands of times their own mass, which was higher than synthetic SAPs of acrylic acid and vinyl alcohol [32,33]. PGlu has been proven to resist drought and promote crop growth as a soil water retainer [13,20]. However, studies on the slow-release potential of PGlu as a coating material in rice systems are lacking.

Due to the large number of carboxyl groups in the branched chain, the structure of SAPs by PGlu is relatively loose and densification and salt tolerance are insufficient [23,24], such as in Figure 1. Therefore, when PGlu is used as a coating material in a rice system, the slow-release period of SRF is short and modification is necessary. Diatomite is an inorganic mineral material with large specific surface area and porous structure [15]. Diatomite is an ideal natural modifier for SAPs due to its low mining cost and no environmental risk. Graft copolymerization of SAPs with diatomite can improve gel strength and salt resistance by providing a large number of silanol groups [34]. The interpenetrating polymer network (INP) formed by chemically forced cross-linking two SAPs was an essential area of SAP blend modification [35–37]. Compared to single SAPs, INP has unique advantages in water absorption and salt resistance [38,39]. However, the preparation of PGlu-based IPN and its slow-release effect in rice systems remained unclear. Biochar is a carbon-rich product obtained by pyrolysis of biomass materials at high temperatures and oxygen-limited conditions [14,40,41].

Biochar has a well-developed pore structure, high cation exchange capacity, and abundant surface functional groups [25,42]. When applied to soil, biochar not only improves the soil structure but also provides a storage place and improves the retention of water and fertilizer [14,43]. Co-coated SRFs consisting of biochar as an inner coating with SAPs as an outer coating are expected to further enhance the slow-release effect of fertilizers. Improvement of the slow-release effect has the potential to mitigate large-scale environmental degradation caused by N loss from agricultural fields, such as acidification and eutrophication, and to improve fertilizer use efficiency with lower cost. Therefore, it is meaningful to evaluate the practical effects of different modifications and enhancements in rice systems.

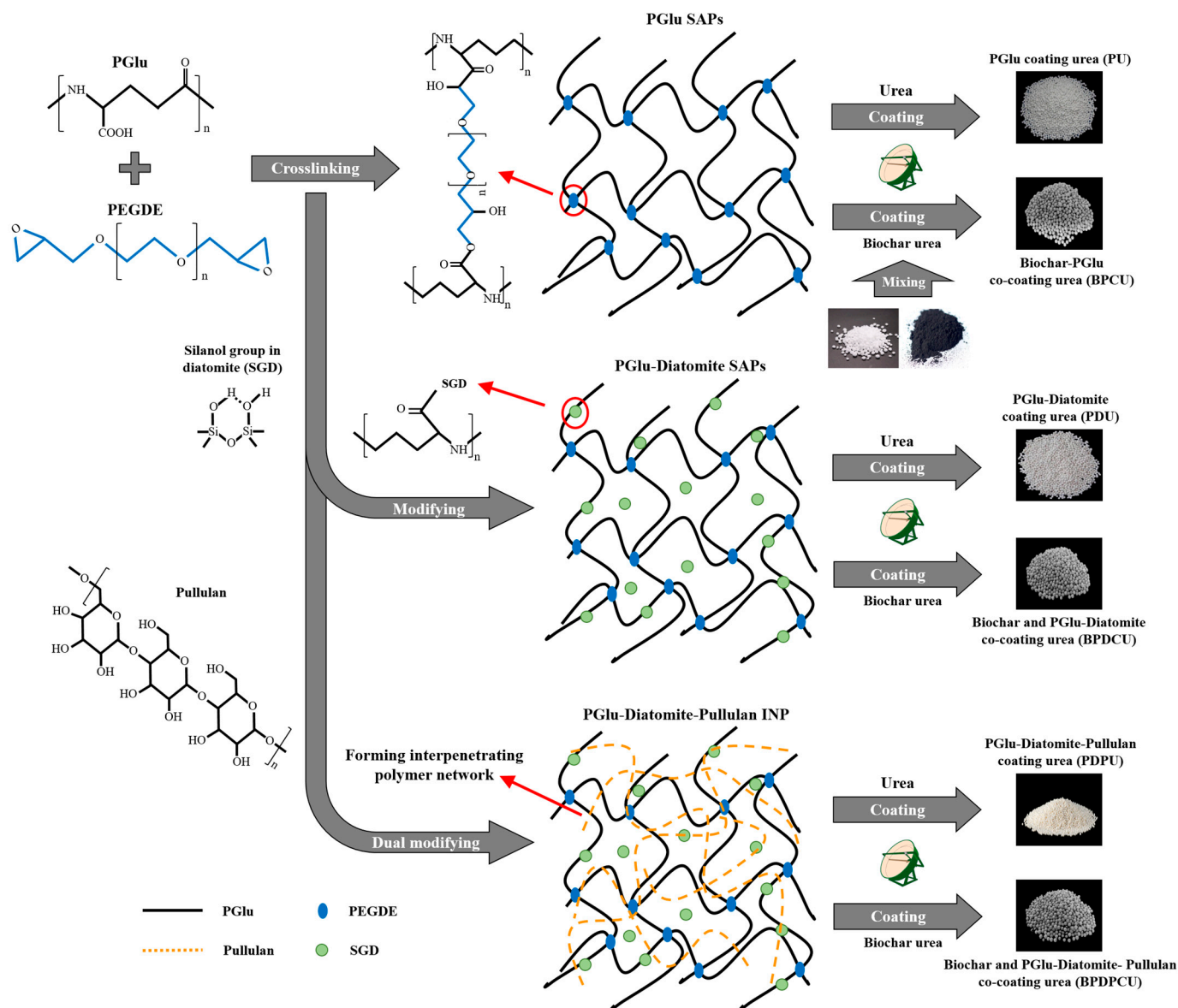


**Figure 1.** Synthesis and modification pathway of  $\gamma$ -polyglutamic (PGlu) acid-coated fertilizers.

In this study, natural SAPs were constructed with PGlu and progressively modified by diatomite and pullulan polysaccharide. Through the coating of urea and biochar-urea with modified SAPs, three mono-layer coated SRFs and three double-layer co-coated SRFs were established (Figure 1). Furthermore, the effects of different SRFs on rice growth and fertilizer N budget were evaluated based on a 150-day rice leaching column incubation experiment with  $^{15}\text{N}$  isotope tracer technique. Our specific objectives include to (1) explore the effect of different modified steps on the properties of coating materials; (2) evaluate the response of the rice growth to modified SRFs; and (3) analyze the change in nitrogen budget in different modified SRF treatments.

## 2. Materials and Methods

### 2.1. Preparation of Coated Urea

In this study, a total of six types of coated fertilizers were prepared, and the preparation process is shown in Figure 1. Monolayer coating types included PGlu urea (PU), PGlu-diatomite urea (PDU), and PGlu-diatomite-pullulan urea (PDPU). Pullulan denotes pullulan polysaccharide, an extracellular water-soluble polysaccharide with good film-forming properties. Double-layer coating types included biochar and PGlu co-coated urea

(BPCU), biochar and PGlu–diatomite co-coated urea (BPDCU), and biochar and PGlu–diatomite–pullulan co-coated urea (BPDPUCU). All raw materials involved in this study are listed in Table 1.

**Table 1.** Description of the raw materials used in this study.

Full Name	Abbreviation	Source	Description
$\gamma$ -polyglutamic acid	PGlu	Nanjing Xinkai Biotechnology Co., Ltd. (Nanjing, China)	Molecular weight = 1.1 million Da, analytical purity > 95%
Pullulan polysaccharide	Diatomite	Sinopharm Chemical Reagent Co., Ltd. (Shanghai, China)	Median particle size = 22 $\mu\text{m}$ , BET specific surface area = 36.7 $\text{m}^2 \text{g}^{-1}$ , analytical purity > 99%
Pullulan	Pullulan	Sinopharm Chemical Reagent Co., Ltd.	Molecular weight = 0.3 million Da, analytical purity > 99%
Poly (ethylene glycol) diglycidyl ether	PEGDE	Sinopharm Chemical Reagent Co., Ltd.	Molecular weight = 1000 Da, analytical purity > 99%
Biochar	Biochar	Self-made with rice straw	Biochar was prepared using rice straw pyrolyzed for 4 h at a temperature of 550 $^{\circ}\text{C}$ and a heating rate of 4 $^{\circ}\text{C} \text{min}^{-1}$
Urea	Urea	Sinopharm Chemical Reagent Co., Ltd.	Analytical purity > 99.8% (Guaranteed Reagent)
$^{15}\text{N}$ -Urea	$^{15}\text{N}$ -Urea	Wuhan Newradar Trade Company Limited (Wuhan, China)	CAS: 2067-80-3, Analytical purity > 99.5% (Analytical Reagent), $^{15}\text{N}$ abundance = 99 atoms %

The PGlu SAPs was prepared by dissolving PGlu (wt% = 5–30%) in ultrapure water (pH = 3–8%) at 50  $^{\circ}\text{C}$  to make a homogeneous and stable solution under constant magnetic stirring [13,18]. The solution was added with 5–30% (wt%) PEGDE as a crosslinking agent and the hydrogel was generated at 200–700 W microwave power. The made hydrogels were washed 5–10 times with distilled water and anhydrous ethanol, respectively, to remove unreacted PGlu. Finally, the hydrogel was vacuum-dried, ground, and passed through a 100-mesh sieve.

The PU was prepared by placing the urea particles in a disc granulator (with a diameter of 0.9 m, dip angle of 35 $^{\circ}$ , and speed of 30 r/min) and spraying an appropriate amount of deionized water onto the urea particles. When the surface of the urea particles appeared to be slightly adherent, PGlu SAPs powder (wt% = 10%) was slowly sprinkled in and rotated until the urea particles were fully encapsulated. The above coating process was repeated to increase the coating thickness and obtain the monolayer coated urea PU. The PDU was made by adding diatomite (wt% = 5–40%) to the PGlu solution, and the other processes of making and coating were the same as PU. The PDPU were prepared by adding pullulan (wt% = 10–60%) into PGlu–diatomite mixed solution, and the other processes of making and coating were the same as PU.

Double-layer coated urea was prepared by generating a fertilizer core biochar-urea (BU) [14,25]. Biochar was mixed with urea (1:20 ( $w/w$ )), added to sufficient deionized water, and stirred for 24 h. The mixture was dried at 55  $^{\circ}\text{C}$  to prepare BU. Then, SAPs were used as the outer coating, biochar, as the inner coating, and BU as the fertilizer core for granulation and coating. The granulation and coating process were the same as that of monolayer coated urea.

## 2.2. Characterization of Coating Materials

Water absorbency can sensitively capture the response of the material's structural tightness and salt resistance to changes in synthesis conditions [15]. Thus, water absorbency was used to determine the optimal conditions for SAP synthesis. The water absorption ratio

of the coating material is the percentage change in the mass of the material after absorbing 3 h in deionized water and 0.9% NaCl solution [20]:

$$WA = \frac{m_1 - m_2}{m_1} \quad (1)$$

where  $WA$  is the water absorption ratio and  $m_1$  and  $m_2$  are the before and after mass of coating material.

The water-holding capacity was determined by placing the water-absorbed coating material at 80 °C and periodically measuring the mass change in the material before and after heating [44]:

$$WH = \frac{m_2}{m_1} \times 100\% \quad (2)$$

where  $WH$  is the water holding ratio and  $m_1$  and  $m_2$  are the before and after mass of coating material.

The slow-release effect of fertilizer was determined by deionized water extraction [15,25]. Nylon nets containing 5.000 g of urea fertilizer were immersed in 250 mL of deionized water and incubated at 25 °C at a constant temperature. Nylon nets were taken out daily, the N concentration in deionized water was analyzed, and the nets were immersed in fresh deionized water to cycle through the analysis steps. Finally, the cumulative nitrogen release from the fertilizer was calculated for 14 days.

A Fourier infrared spectrometer (FTIR, INVENIOR, Bruker, Billerica, MA, USA) was used to analyze the functional group changes of the samples; the scanning range was 500–4000  $\text{cm}^{-1}$ , spectral resolution was 4  $\text{cm}^{-1}$ , and scanning speed was 0.2  $\text{cm s}^{-1}$ .

The thermal stability of the hydrogel was determined using a thermogravimetric analyzer (TGA-Q5000IR, TA, New Castle, DE, USA) [15]. The mass loss of the coating material between 25 and 650 °C was measured in a constant stream of  $\text{N}_2$  at a temperature increase rate of 10 °C  $\text{min}^{-1}$ .

The biodegradability of the coating material was assessed using the soil burial method [45]. Briefly, 5.000 g of coating material was buried 5 cm into the soil using a nylon mesh bag and maintained at a constant soil temperature and humidity. The nylon net was taken out every 6 days, washed, dried, and weighed. The assay was repeated up to 90 days.

### 2.3. Description of the Rice-Leaching Column Incubation Experiment

A rice-leaching column incubation experiment was conducted at the scientific research dry shelter of Northwest A&F University in Yangling, Shaanxi (108°04'10" E, 34°15'46" N). The study period was from May 2023 to October 2023, a total of 180 days. The leaching column was made of PVC pipe with 18 cm diameter and 100 cm total length (Figure 2a). The 10–60 cm section of the leaching column was filled with sample soil and 0–10 cm was used for flooding treatment. The strainer was fixed at a depth of 60 cm in the leaching column to filter the leachate and prevent soil loss. The leaching column was empty at 60–100 cm and a 1.5 L wide-mouth bottle and funnel were placed to collect the leachate.

The sample soil was bleached paddy soil, and the soil was taken from Maanshan, Anhui Province (118°33'36" E, 31°40'12" N). The soil pH was  $5.3 \pm 0.4$ , the soil organic carbon (SOC) amounted to  $1.5 \pm 0.2\%$ , the total nitrogen content amounted to  $0.108 \pm 0.013\%$ , the available phosphorus amounted to  $5.6 \pm 0.21 \text{ mg kg}^{-1}$ , the available potassium amounted to  $69.3 \pm 8.2 \text{ mg kg}^{-1}$ , and the cation exchange capacity was  $10.3 \pm 1.3 \text{ mg kg}^{-1}$ . Soil was sieved through 2 mm holes after sampling and evenly filled to 10–60 cm of each leaching column.

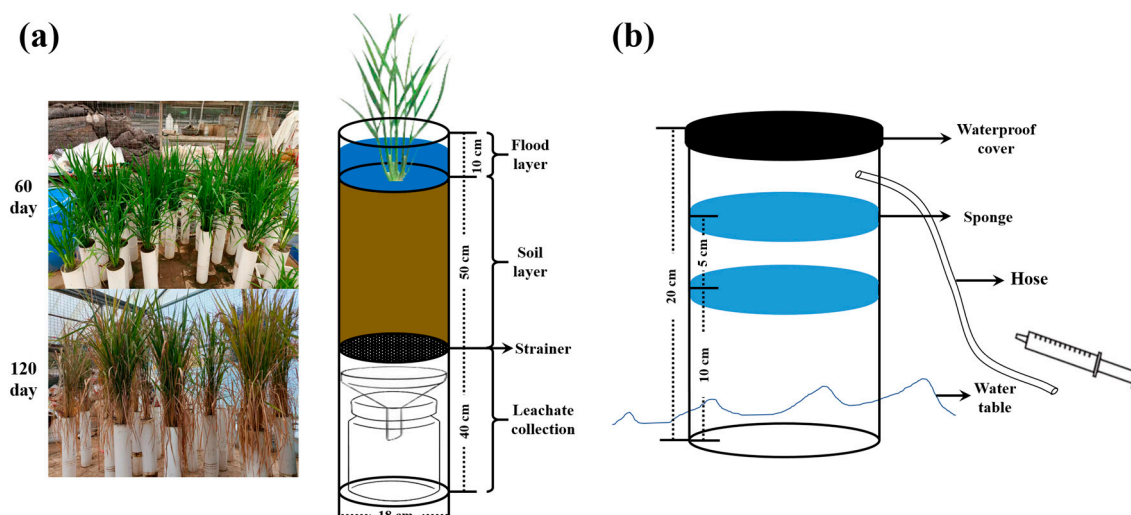


**Figure 2.** Description of rice-leaching column incubation experiment (a) and closed-chamber sponge absorption system (b).

#### 2.4. Treatment Design of Incubation Experiment

Seven treatments were set up, including a conventional urea treatment (U) and six coated fertilizers, which were PU, PDU, PDP, BPCU, BPDCU, and BPDPCU. Each treatment was replicated three times. Other nutrient inputs and irrigation management were the same between treatments. During the rice growth period, drip irrigation equipment was used to continuously irrigate the treatments, and the depth of rice water and rice field sunning were uniformly controlled according to rice growth. Urea with  $^{15}\text{N}$  abundance of 99 atoms % was used as a tracer in this incubation experiment (2067-80-3, Newradar, Wuhan, China).

#### 2.5. Measurement of Fertilizer Nitrogen Loss

During the first 15 days of the experiment, all leachates were collected every three days and the  $^{15}\text{N}$  concentration in the leachate was measured by Elemental analyzer-Isotope ratio mass spectrometer (EA-IRMS, DELTA V, Thermo Fisher, Waltham, MA, USA) [46,47]. Then, they were measured every 7 days from 16 to 64 days and every 14 days after 65 days.

$^{15}\text{N}_2\text{O}$  and  $^{15}\text{NH}_3$  from soil were collected by closed-chamber sponge absorption method (Figure 2b) [48]. The top of the chamber was sealed and the bottom was inserted into the soil. A hose was set up 2 cm from the top of the chamber with a syringe attached to collect the  $^{15}\text{N}_2\text{O}$ . Sponges with 3.0 cm thickness moistened with glycerol phosphate (phosphoric acid/glycerol = 5:4) were placed at 10 and 15 cm of the chamber for collecting  $^{15}\text{NH}_3$ . At the time of gas collection, a 60 mL syringe was used to quickly collect the gas through the hose and then the gas was quickly transferred to a 100 mL aluminum molded gas sample bag and sealed for direct measuring of  $^{15}\text{N}_2\text{O}$ . Immediately after, the sponges in the collection chamber were removed and quickly stored in a self-sealing bag with 200 mL  $1 \text{ mol L}^{-1}$  KCl and shaken for 1 h for analyzing  $^{15}\text{NH}_3$ .  $^{15}\text{N}_2\text{O}$  emission rate was determined by Gas Chromatography-Mass Spectrometer (GC-MS, TQ8050, Shimadzu, Tokyo, Japan).  $^{15}\text{NH}_3$  volatilization rate was analyzed by EA-IRMS.

The nitrogen fraction derived from fertilizer (f) in the leachate,  $\text{N}_2\text{O}$  or  $\text{NH}_3$ , was calculated as follows [49,50]:

$$f = \frac{\left( {}^{15}_{\text{Sample}}\text{N atom\%} - {}^{15}_{\text{control}}\text{N atom\%} \right) \times 100}{\left( {}^{15}_{\text{fertilizer}}\text{N atom\%} - {}^{15}_{\text{control}}\text{N atom\%} \right)} \quad (3)$$

where  ${}^{15}_{\text{Sample}}\text{N atom\%}$  and  ${}^{15}_{\text{control}}\text{N atom\%}$  are the  $^{15}\text{N}$  enrichment with and without nitrogen fertilizer and  ${}^{15}_{\text{fertilizer}}\text{N atom\%}$  is the  $^{15}\text{N}$  enrichment in different nitrogen fertilizers.

The content of fertilizer-derived nitrogen ( $^{FD}N$ ) in the leachate,  $N_2O$  or  $NH_3$ , was calculated with the following equation [51,52]:

$$^{FD}N = \frac{N_{pool} \times f}{100} \quad (4)$$

where  $N_{pool}$  is the amount of nitrogen in the leachate,  $N_2O$  or  $NH_3$ .

The rate ( $mg\ m^{-2}day^{-1}$ ) of  $^{FD}NH_3$  volatilization and  $^{FD}N_2O$  emission are all the collected  $^{FD}N$  content divided by the time, and the total  $^{FD}N$  loss is the sum of the three.

### 2.6. Determination of Biomass and Plant Nitrogen Uptake

The biomass was harvested on the 150th day of the culture experiment. Roots, straw, and grain were separated, killed ( $105\ ^\circ C$ , 2 h), dried ( $65\ ^\circ C$ , 48 h), and weighed.  $^{15}N$  content in each plant fraction was analyzed using EA-IRMS [47,53]. The content of fertilizer-derived nitrogen in each plant fraction was calculated with Equations (3) and (4).

### 2.7. Analysis of Soil Nitrogen Residues

Soil samples were collected layer by layer from 0 to 50 cm depth on days 5, 12, 26, 40, 68, 96, 124, and 180 using a micro soil auger (3.5 cm diameter). Soil total  $^{15}N$  was determined by EA-IRMS [51,54]. Soil ammonium nitrogen was leached with  $2\ mol\ L^{-1}$  KCl, and soil nitrate nitrogen was leached with saturated  $CaSO_4$ , and both were analyzed by EA-IRMS [55,56]. The content of fertilizer-derived nitrogen in each soil fraction was also calculated with Equations (1) and (2). Soil available nitrogen was the sum of ammonium nitrogen and nitrate nitrogen. The soil  $^{FD}N$  stock (S) in each component (total, available, ammonium, and nitrate) was calculated according to Equation (5) [57]:

$$S = \int_{i=1}^n C_i \times d_i \times BD_i \quad (5)$$

where  $C_i$  is N concentration in soil layer  $i$ ,  $d_i$  is soil layer depth, and  $BD_i$  is soil bulk density. Moreover, Soil  $^{FD}N$  residual ratio is the proportion of soil total  $^{FD}N$  stock to total  $^{FD}N$  application.

### 2.8. Data Analysis

Because some of the data did not satisfy the F test and normality, nonparametric tests were used to verify the significance of between the samples. Specifically, the Mann–Whitney U test ( $p < 0.05$ ) was employed to analyze the significance of the two samples and the Kruskal–Wallis H test and the Dunn’s test (multiple comparisons,  $p < 0.05$ ) were adopted in the comparison of multifactorial, multilevel samples. Person correlation analysis was used to calculate the correlation coefficients (r) between all paired variables, and a significant correlation was indicated when  $p < 0.05$ . Statistical analyses were all performed using the statsmodels (version 0.12.2) package in Python 3.8.

## 3. Results

### 3.1. Effect of Modification on Slow-Release Fertilizer

The effect of different reaction conditions on water absorbency by SAPs is illustrated in Figure 3. The maximum water absorbency of SAPs synthesized using PGLu in this study ranged from 548 to 563  $g\ g^{-1}$  in deionized water and from 47.36 to 48.68%  $g\ g^{-1}$  in 0.9% NaCl solution, respectively (Figure 3a–d). The conditions for maximum water absorbency were the concentration of PGLu at  $160\ g\ L^{-1}$ , the reaction solution pH at 4, the microwave radiation power at 500 w, and the cross-linking agent at 20%, respectively. The addition of diatomite further increased the water absorbency of SAPs, with maximum absorbency of  $601 \pm 38.2\ g\ g^{-1}$  in deionized water and  $52.5 \pm 4.2\ g\ g^{-1}$  in 0.9% NaCl solution, respectively (Figure 3e). The improvement in water absorbency by pullulan was

superior to that of diatomite, with maximum absorbency of  $652 \pm 38.2 \text{ g g}^{-1}$  in deionized water and  $56.2 \pm 4.7 \text{ g g}^{-1}$  in 0.9% NaCl solution, respectively (Figure 3f).

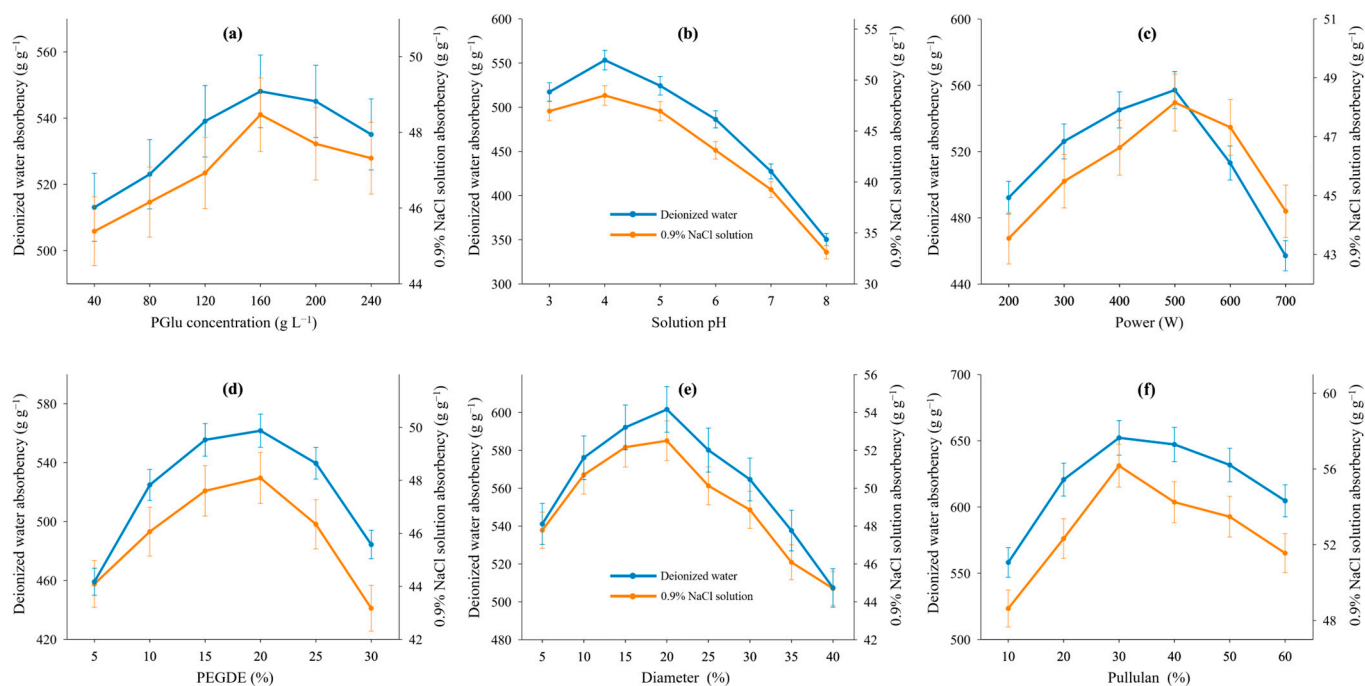


**Figure 3.** Effect of PGLu concentration (a), solution pH (b), microwave power (c), the quality ratio of PEGDE to PGLu (d), the quality ratio of diameter to PGLu (e), and the quality ratio of pullulan to PGLu (f) on water absorbency of SAPs.

Modification by diatomite and pullulan significantly improved the stability and slow-release capacity of the fertilizers (Figure 4). The combined modification of diatomite and pullulan significantly increased the water absorbency of PU and BPCU by  $21.6 \pm 3.2\%$  and  $18.9\% \pm 2.5\%$  (Figure 4a). Biochar, diatomite, and pullulan all improved the water-holding capacity by  $13.6 \pm 2.4\%$ ,  $27.3 \pm 3.7\%$ , and  $43.2 \pm 3.5\%$  (Figure 4b). Accumulated N release indicated that double-layer coating types had better slow release. The N residues of BPCU, BPDCU, and BPDPCU after 14 days of immersion were  $16.1 \pm 4.3\%$ ,  $21.3 \pm 6.1\%$ , and  $26.4 \pm 4.4\%$ , respectively (Figure 4c). In FTIR spectra, the stretching vibration peaks of Si–O–Si at  $473$  and  $1055 \text{ cm}^{-1}$  observed in the PDU and PDCU demonstrated that diatomite was successfully integrated with SAPs. The broadening  $-\text{RCOO}$  vibration peaks at  $1411 \text{ cm}^{-1}$  and  $-\text{OH}$  vibration peaks at  $3574 \text{ cm}^{-1}$  indicated the construction of PGLu–pullulan INP through hydrogen bonding (Figure 4d). The modification significantly improved the thermal stability of the fertilizer, which was attributed to the incorporation of thermally stable materials, diatomite and biochar, as well as the formation of more stable chemical bonds between the polymers (Figure 4e). Furthermore, biodegradation showed that the modification of diatomite and pullulan did not hinder the degradation of SAPs (Figure 4f).

### 3.2. Rice Growth and Plant Nitrogen Uptake

Comparison of rice growth and fertilizer nitrogen (<sup>FD</sup>N) uptake for each treatment are shown in Figures 5 and 6. Compared to conventional urea, PDCU, BPCU, BPDCU, and BPDPCU increased significantly ( $p < 0.05$ ) aboveground and grain biomass by 5.43–10.01 and 4.85–9.88% (Figure 4a,c). The significant increase ( $p < 0.05$ ) in belowground was shown only for BPDCU ( $9.11 \pm 3.7\%$ ) (Figure 4b). Compared to urea treatment, PDU and PDCU of monolayer coated urea increased significantly by  $6.6 \pm 2.4$  and  $13.3 \pm 4.2\%$  plant N uptake, and, for double-layer coated urea, all increased significantly plant N uptake by 10.1 to 17.2% ( $p < 0.05$ ). Moreover, the double-layer coated urea with modified SAPs could

further improve N use efficiency, and the plant N uptake of BPDPCU was also higher than all monolayer coated urea (Figure 5).

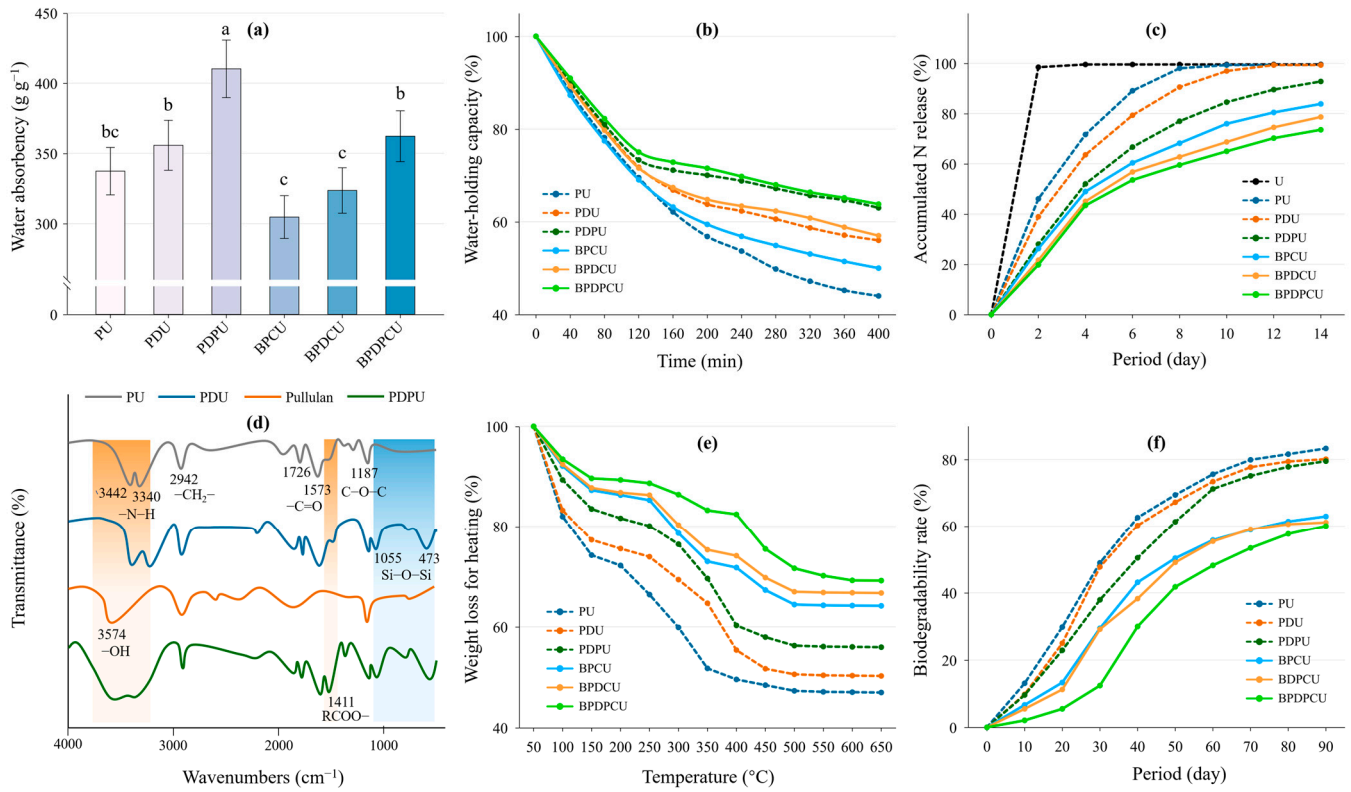


**Figure 4.** Effect of modification on fertilizer water absorbency (a), water holding (b), slow-release effect (c), FTIR spectra (d), thermal stability (e), and biodegradability rate (f). Note: U is urea, PU is PGLu coated urea, PDU is PGLu–diatomite coated urea, PDPU is PGLu–diatomite–pullulan coated urea, and BPCU, BPDCU, and BPDPCU are PGLu, PGLu–diatomite, and PGLu–diatomite–pullulan co-coated biochar urea. Different lower-case letters indicate significance  $p < 0.05$  between treatments.

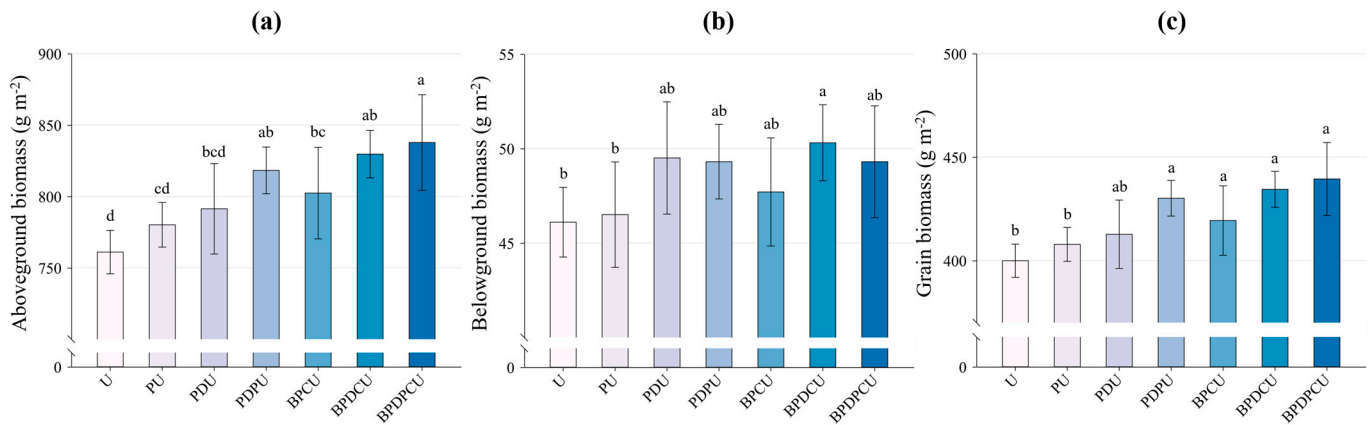


**Figure 5.** Effect of coated urea on rice aboveground (a), belowground (b), and grain biomass (c). Note: U is urea, PU is PGLu coated urea, PDU is PGLu–diatomite coated urea, PDPU is PGLu–diatomite–pullulan coated urea, and BPCU, BPDCU, and BPDPCU are PGLu, PGLu–diatomite, and PGLu–diatomite–pullulan co-coated biochar urea. Different lower-case letters indicate significance  $p < 0.05$  between treatments.

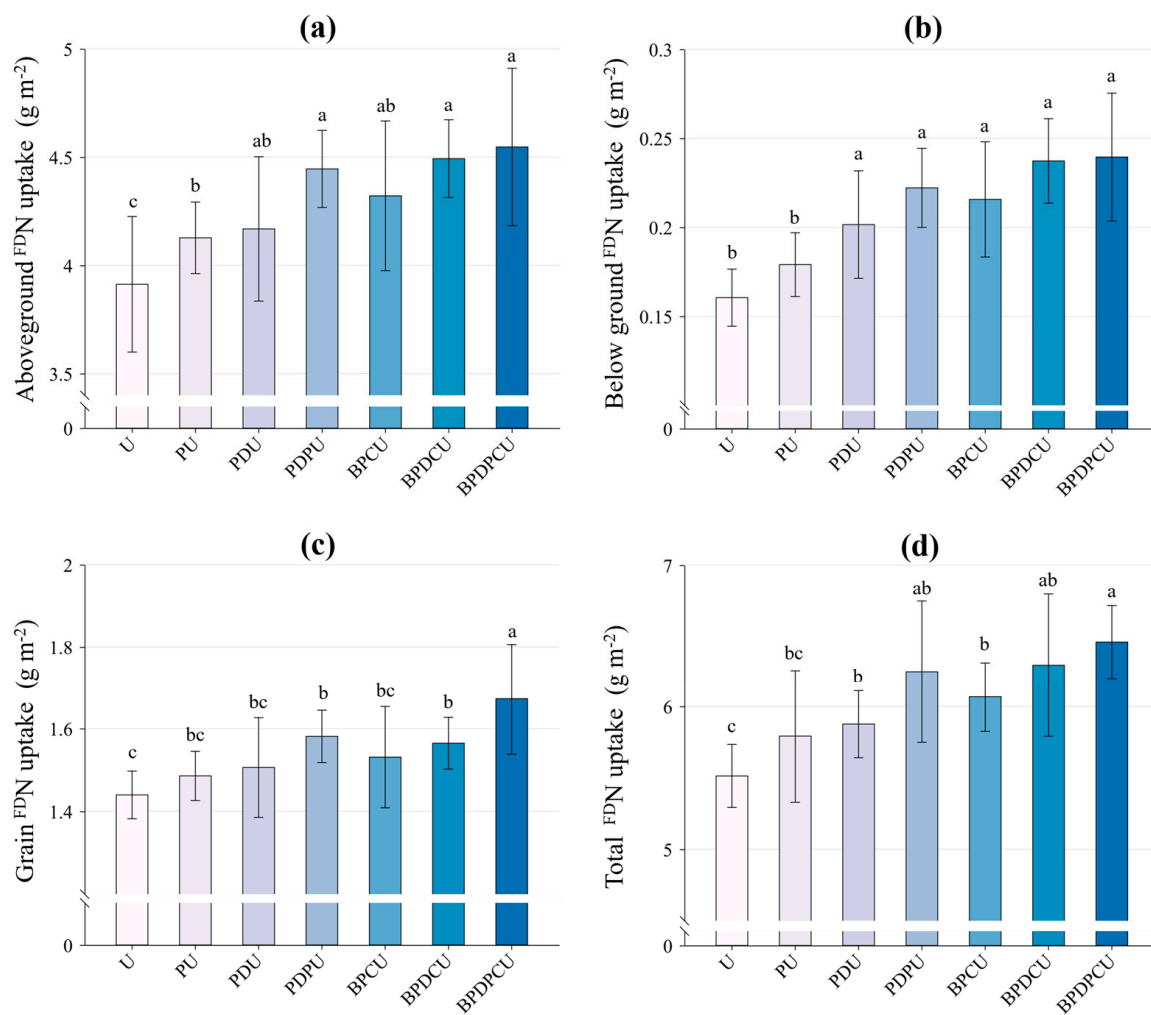


**Figure 6.** Fertilizer-driven nitrogen (<sup>FDN</sup>) in rice aboveground (a), belowground (b), and grain (c) and total uptake (d). Note: U is urea, PU is PGLu coated urea, PDU is PGLu–diatomite coated urea, PDP is PGLu–diatomite–pullulan coated urea, and BPCU, BPDCU, and BPDPCU are PGLu, PGLu–diatomite, and PGLu–diatomite–pullulan co-coated biochar urea. Different lower-case letters indicate significance  $p < 0.05$  between treatments.

### 3.3. Fertilizer-Derived Nitrogen in Soil

Soil profile data indicated that PDP, BPCU, BPDCU, and BPDPCU could retain <sup>FDN</sup> in the soil for a longer period (Figure 7), which significantly ( $p < 0.05$ ) increased <sup>FDN</sup> in the soil profile from 14 to 56 days. Total soil <sup>FDN</sup> stock further revealed (Figure 8a) that PDP, BPCU, BPDCU, and BPDPCU significantly ( $p < 0.05$ ) increased average <sup>FDN</sup> stock by  $20.9 \pm 6.2$ ,  $24.8 \pm 5.3$ ,  $31.2 \pm 6.8$ , and  $37.9 \pm 7.4\%$  during 14–56 days. Soil available (ammonium and nitrate) <sup>FDN</sup> stocks further indicated (Figure 8b,c) that double-layer co-coated urea can release nutrients more slowly and permanently than conventional urea. Ammonium nitrogen of PDP, BPCU, BPDCU, and BPDPCU was significantly higher with conventional urea at 28 and 56 days, with average increases of  $3.5 \pm 1.2$ ,  $5.3 \pm 2.2$ ,  $5.5 \pm 2.1$ , and  $6.5 \pm 2.4$  g cm<sup>-1</sup>. Pullulan-modified and double-layer co-coated also significantly slowed down the fertilizer N digestion rate. Soil nitrate <sup>FDN</sup> content of PDP, BPCU, BPDCU, and BPDPCU was significantly lower than that of the conventional urea treatment from 0 to 14 days, with average decreases of  $22.1 \pm 4.6$ ,  $31.1 \pm 3.8$ ,  $34.4 \pm 5.2$ , and  $35.6 \pm 4.5$  g% (Figure 8c).

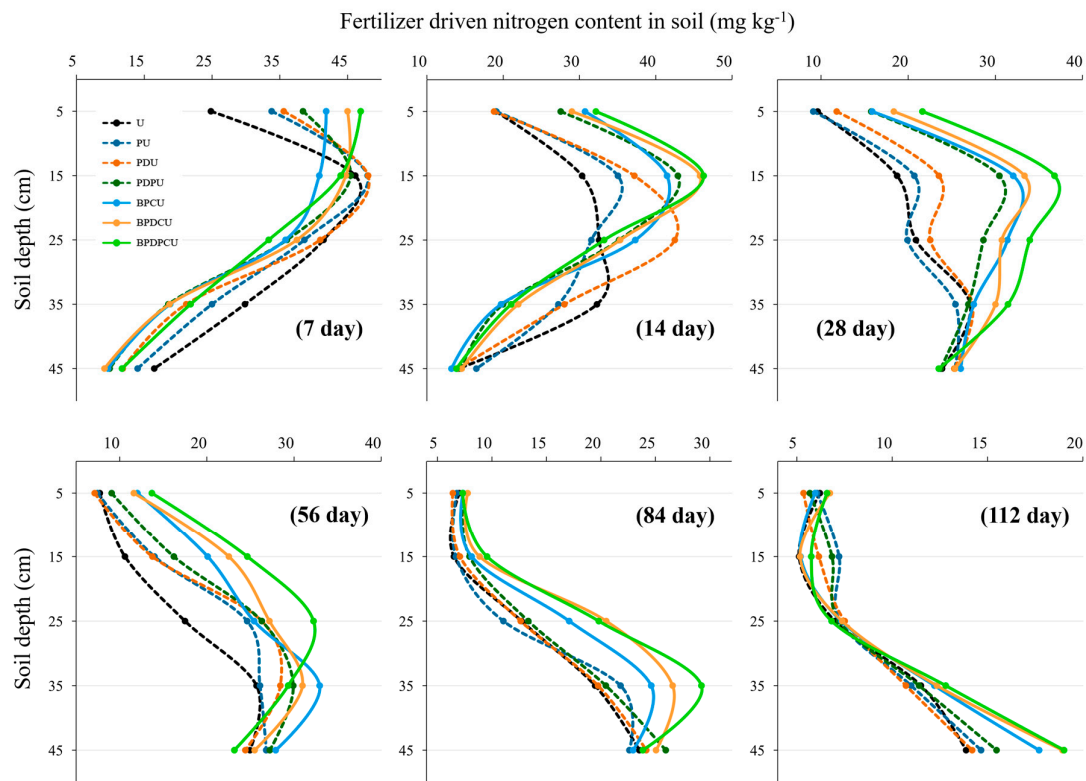


**Figure 7.** The distribution of average fertilizer-derived nitrogen in 0–50 cm soil profile during 150 days. Note: U is urea, PU is PGLu coated urea, PDU is PGLu–diatomite coated urea, PDP is PGLu–diatomite–pullulan coated urea, and BPCU, BPDCU, and BPDPCU are PGLu, PGLu–diatomite, and PGLu–diatomite–pullulan co-coated biochar urea.

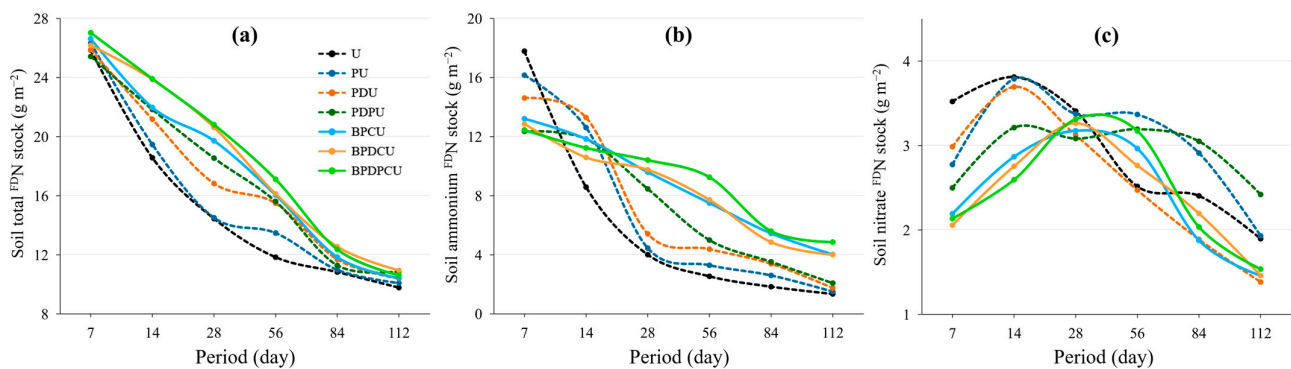


**Figure 8.** The average of soil total fertilizer-derived nitrogen (<sup>FDN</sup>) stock (a), ammonium <sup>FDN</sup> stock (b), and nitrate <sup>FDN</sup> stock (c) in the different treatments. Note: U is urea, PU is PGLu coated urea, PDU is PGLu–diatomite coated urea, PDP is PGLu–diatomite–pullulan coated urea, and BPCU, BPDCU, and BPDPCU are PGLu, PGLu–diatomite, PGLu–diatomite–pullulan co-coated biochar urea.

### 3.4. Fertilizer-Derived Nitrogen Loss

Continuous monitoring for 150 days indicated that coated urea significantly reduced <sup>FDN</sup> losses by 7.5–30.4% ( $p < 0.05$ ), and 51.2–70.5% of this reduction was contributed by a decrease in <sup>FDN</sup> leaching (Figure 9 and Table 2). PDP, BPDCU, and BPDPCU significantly ( $p < 0.05$ ) reduced the pre-existing leachate <sup>FDN</sup> content in the rice-leakage system, and the total <sup>FDN</sup> leaching decreased by  $25.5 \pm 8.3$ ,  $27.3 \pm 8.7$  and  $33.2 \pm 9.5\%$  during the total growth period (Figure 9a). PDP, BPDCU, and BPDPCU reduced the <sup>FDN</sup><sub>2</sub>O emission rate from 7 to 28 days, but total <sup>FDN</sup><sub>2</sub>O emission throughout the growth period was not significantly reduced (Figure 9b). During 7 to 42 days, PDP, BPCU, BPDCU, and BPDPCU

reduced significantly the  $^{FD}NH_3$  volatilization rate ( $p < 0.05$ ), and total  $^{FD}NH_3$  volatilization during the growing period was significantly reduced by  $65.7 \pm 18.5$ ,  $82.9 \pm 21.3$ ,  $74.2 \pm 21.6$ , and  $78.7 \pm 17.4\%$  (Figure 9c).

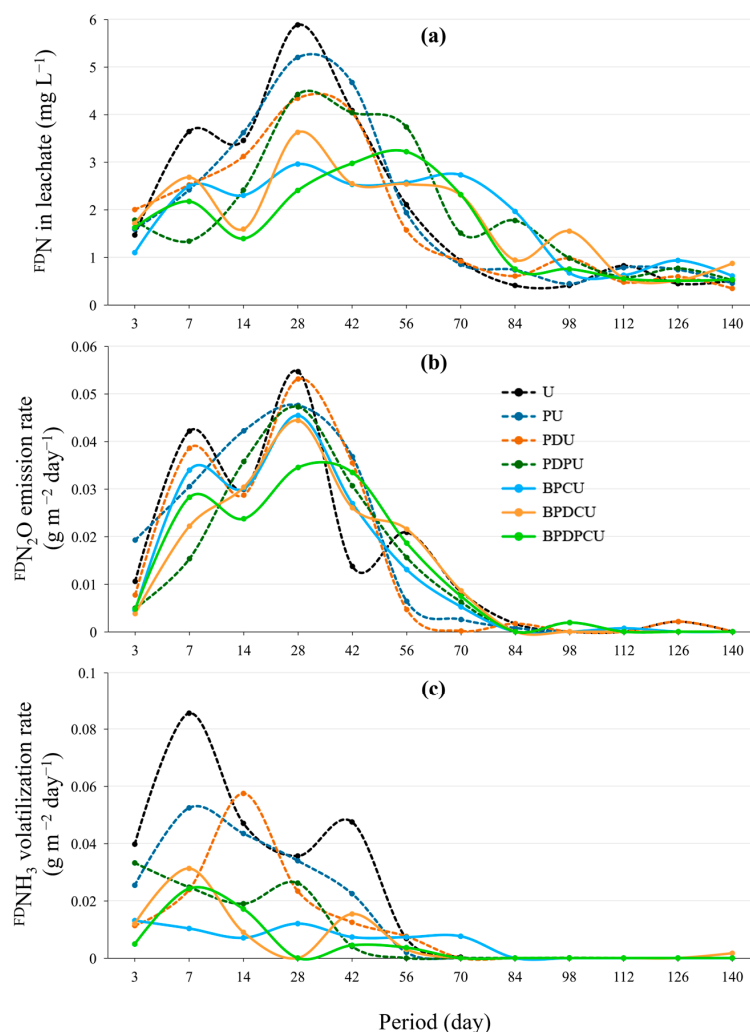


**Figure 9.** The average of fertilizer-derived nitrogen ( $^{FD}N$ ) leaching (a),  $^{FD}N_2O$  emissions (b), and  $^{FD}NH_3$  volatilization (c) in the different treatments. Note: U is urea, PU is PGlu coated urea, PDU is PGlu–diatomite coated urea, PDPU is PGlu–diatomite–pullulan coated urea, and BPCU, BPDCU, and BPDPCU are PGlu, PGlu–diatomite, and PGlu–diatomite–pullulan co-coated biochar urea.

**Table 2.** Fertilizer-driven nitrogen ( $^{FD}N$ ) element budget. Note: U is urea, PU is PGlu coated urea, PDU is PGlu–diatomite coated urea, PDPU is PGlu–diatomite–pullulan coated urea, and BPCU, BPDCU, and BPDPCU are PGlu, PGlu–diatomite, and PGlu–diatomite–pullulan co-coated biochar urea. Different lower-case letters indicate significance  $p < 0.05$  between treatments.

Treatment	Plant $^{FD}N$ Uptake ( $g\ m^{-2}$ )	$^{FD}N$ Soil Residue ( $g\ m^{-2}$ )	$^{FD}N$ Loss ( $g\ m^{-2}$ )			Recovery Ratio (%)
			Leaching	$N_2O$	$NH_3$	
U	5.46 <sup>b</sup> ± 0.7	9.63 <sup>b</sup> ± 2.1	7.29 <sup>a</sup> ± 2.2	3.12 <sup>a</sup> ± 0.85	2.04 <sup>a</sup> ± 0.72	91.8 <sup>a</sup> ± 12.3
PU	5.79 <sup>b</sup> ± 1.4	10.8 <sup>ab</sup> ± 1.6	6.69 <sup>a</sup> ± 1.7	3.27 <sup>a</sup> ± 0.57	1.56 <sup>a</sup> ± 0.38	91.3 <sup>a</sup> ± 10.7
PDU	5.88 <sup>ab</sup> ± 1.3	10.38 <sup>ab</sup> ± 2.0	6.51 <sup>a</sup> ± 1.5	3.18 <sup>a</sup> ± 1.12	1.26 <sup>ab</sup> ± 0.52	90.7 <sup>a</sup> ± 12.8
PDPU	6.36 <sup>ab</sup> ± 1.4	10.86 <sup>a</sup> ± 1.5	5.43 <sup>bc</sup> ± 1.8	3.36 <sup>a</sup> ± 0.48	1.02 <sup>b</sup> ± 0.41	90.1 <sup>a</sup> ± 15.0
BPCU	6.27 <sup>ab</sup> ± 2.1	10.41 <sup>ab</sup> ± 1.8	6.06 <sup>ab</sup> ± 1.5	2.88 <sup>a</sup> ± 0.57	1.06 <sup>b</sup> ± 0.73	88.9 <sup>a</sup> ± 11.8
BPDCU	6.48 <sup>a</sup> ± 1.3	10.92 <sup>a</sup> ± 2.3	5.31 <sup>bc</sup> ± 1.9	3.15 <sup>a</sup> ± 0.90	0.99 <sup>b</sup> ± 0.43	89.5 <sup>a</sup> ± 11.5
BPDPCU	6.69 <sup>a</sup> ± 1.5	11.28 <sup>a</sup> ± 2.2	4.86 <sup>c</sup> ± 1.8	3.02 <sup>a</sup> ± 0.69	0.79 <sup>b</sup> ± 0.25	88.8 <sup>a</sup> ± 14.7

## 4. Discussion

### 4.1. Enhancement of PGLu SAP Slow-Release Effect by Diatomite and Pullulan

Current research on organic coating materials mainly focuses on synthetic SAPs such as polyacrylic acid and polyvinyl alcohol [11,17]. Due to the relatively stable chemical properties and difficulty being degraded by living organisms, synthetic SAPs may cause a certain amount of pollution to the environment in the process of production and application [37]. Moreover, the raw materials for synthetic SAPs were mainly derived from nonrenewable resources such as petrochemicals, which restricts their environmental friendliness and sustainability [18]. Therefore, it was necessary to study environmentally friendly natural SAPs. In this study, PGLu-based SAPs were fabricated using PEGDE as a cross-linking agent under microwave radiation conditions (Figure 1). The results of this study showed that the best dissolution performance of SAPs was achieved when the concentration of PGLu solution was  $160 \text{ g L}^{-1}$ , the reaction pH was 4, the microwave power was 500 w, and the amount of cross-linker PEGDE was 20% (Figure 3). Reactant and cross-linker dosage were important factors affecting SAPs. Too high a dosage of PGLu and PEGDE would result in too tight cross-linking of the SAPs and thus reduce the water-absorbent properties of the SAPs, while too low a dosage would result in insufficient cross-linking of the SAPs' mesh structure. The optimal reaction pH was acidic because  $\text{H}^+$  can activate free radicals in PEGDE, which, in turn, accelerated the cross-linking reaction [13]. Compared to conventional heating, microwave radiation can accelerate the reaction rate and make the reactants more homogeneous and stable [15]. Microwave radiation of 500 w can effectively improve the swelling properties of SAPs but too high a radiation power can make the cross-linking result too tight and, thus, reduce the water absorption. As a biodegradable SAP, PGLu had a low environmental impact during production and application. The raw materials of PGLu were from a wide range of sources and can be produced in a sustainable way, such as through microbial fermentation [16,20,32]. The production process of PGLu was consistent with the concepts of environmental protection and sustainable development [28,33].

This study demonstrated further that diatomite and pullulan polysaccharides significantly improved the structural stability of PGLu SAPs, which consequently prolonged the slow-release effect of the coated urea (Figure 4c). Diatomite, with unique pore structure and hydrophilicity, can significantly enhance the mechanical properties when added as a filler to the hydrogels [58]. Material characterization revealed that, when diatomite was added at 20%, the water absorbency of SAPs increased by 15% and water holding capacity by 17.3% (Figure 4a,b). Due to the distribution and interaction of diatomite in the hydrogel network structure, it also restricted the swelling behavior of the hydrogel and reduced its volume change in the solvent [59,60]. Diatomite also has a positive effect on the thermal stability of hydrogels (Figure 4e). The interaction of amphiphilic bicontinuous networks improves the thermal degradation behavior of hydrogels, and the incorporation of diatomite further enhances this interaction, thus improving the thermal stability of hydrogels [58,61]. Semi-interpenetrating polymer network (INP) technology can blend polymers that are partially compatible or even incompatible but have complementary properties to form a multiphase structure with microphase separation [62,63]. INP leads to a more complex network structure of the hydrogel, which was able to absorb and retain moisture more efficiently [37]. By introducing hydrophilic groups (e.g., hydroxyl, carboxyl, phosphate groups, etc.), the swelling rate of INP hydrogels can be significantly increased [12,64]. The present results indicated that the semi-interpenetrating network established by pullulan could significantly improve the water absorption and retardation properties of SAPs (Figure 4). When pullulan was added at 30%, the water absorbency of SAPs was significantly increased by 25.3% (Figure 3f). However, excessively high incorporation of pullulan can make the cross-linking of the structure too tight, thus reducing the water absorption property of SAPs. Moreover, the water holding, slow-release effect, and thermal stability of the INP-based modified SAPs were significantly higher than those of the single diatomite modification (Figure 4). By introducing special polymer chains, INP can also make SAPs exhibit environmental sensitivities, such as salt sensitivity through the introduction of sodium alginate and pH

sensitivity through the introduction of chitosan [64]. It can be seen that INP is of great importance for the future in many areas, such as the intelligentization of SAPs and the innovation of controlled-application coated fertilizers.

#### 4.2. Improvement of Crop Growth and Nitrogen Loss by Modified SAPs

Coated urea reduces N leaching, volatilization, and fixation by avoiding direct contact of water-soluble nutrients with soil and crop roots [11,12]. When water enters SAPs, nutrients are dissolved and osmotic pressure rises, prompting the slow diffusion of nutrients through the film into the soil solution, thus continuously being absorbed and utilized by crops [14,25]. However, the enhancement of crop productivity and nutrient use efficiency by natural PGlu-based coated urea was limited due to poor water stability and short slow-release period in rice systems with frequent wet and dry intervals. The results of this study showed that the slow-release effect could be improved by co-coating urea with modified SAPs and biochar, which significantly enhanced rice yield and plant N uptake (Figures 5 and 6). Among the modified treatments, pullulan-based INP was the most effective in increasing crop grain yields and plant nitrogen uptake of in-season fertilizers. Single-layer INP-coated urea PDPU enhanced plant growth and nutrient uptake stronger than double-layer coated BPCU (Figures 5c and 6d). It is evident that INP-coated urea has the potential to further increase crop yields and stabilize regional food security at the same level of N input. The economic benefits from additional yields could also be used to offset the input costs, achieving a virtuous cycle of farmland in terms of economic efficiency. Diatomite not only enhances the SAP stability and slow release of the encapsulated fertilizer but also provides additional available silicon for rice [58,60,61]. Silicon is one of the essential nutrients for plant growth and has a significant impact on plant growth, especially for silica-loving crops such as rice [65,66]. Silicon fertilizer can silicify rice epidermal cells, enhance the strength of cell walls, make stems and leaves erect, reduce shading, and facilitate dense planting [67]. Silicon also increases the chlorophyll content in rice plants and extends the reproductive period of the crop, thereby increasing photosynthetic utilization and promoting plant growth [68]. Moreover, the decomposition of polyglutamic acid can also provide additional small-molecule amino acids to rice to act as a nutrient booster [16,19]. The application of amino acids contributes to facilitating the synthesis of vital plant substances, including chlorophyll, enzymes, and proteins [69]. Amino acids also could promote root development, regulate acidity and alkalinity within the plant body, and enhance resilience to environmental stresses [70]. Therefore, modified PGlu-coated urea with multiple positive benefits is an important option for future nutrient sources in rice systems.

In order to solve food security and achieve high rice yields, nitrogen fertilizer applications have been as high as 100–300 kg ha<sup>-1</sup> annually [71–73]. However, the seasonal utilization of nitrogen fertilizers is relatively low at only 30–50%, while a considerable portion of nitrogen fertilizers are leached or volatilized [2,74,75]. Unused nitrogen fertilizer increases soil acidification, breaks down soil inorganic carbon, and releases greenhouse gases such as CO<sub>2</sub> and N<sub>2</sub>O [4,76–78]. Additional nitrogen fertilizer leaching into the earth's water system can also pollute water resources and trigger a range of environmental problems such as eutrophication of water bodies [72]. The results of this study show that modified double-layer co-coated urea can significantly reduce fertilizer nitrogen losses in rice systems (Figure 9). Soil N dynamics monitoring indicated that pullulan-modified and co-coated urea significantly extended the residence time of N in the soil profile up to the 56th day (Figures 7 and 8a). The prolonged release of fertilizer led to a better matching of nutrient supply to the rice growth cycle, which contributed to a reduction in the number and amount of fertilizer applications. The extended slow-release effect of the fertilizer also significantly reduced N losses at early stages, resulting in a 7.5–30.4% reduction in total fertilizer N losses. Nitrogen losses reduced through co-coated urea are significant for the sustainability of the rice system. Relevant data indicate that more than 10 million tons of nitrogen fertilizer applied in Chinese farming was lost through ammonia volatilization,

nitrous oxide emissions, leaching, and other pathways, accounting for 52% of the nitrogen applied, which is equivalent to more than 20 million tons of urea [73,75,79]. Large amounts of leaching nitrogen not only constrain the farmland resource sustainability but also aggravate the environmental carrying capacity and raise different environmental risks [80,81]. Co-coated urea with modified SAPs and biochar not only significantly reduces the leaching of fertilizer nitrogen, it also changes the form of leached nitrogen so that the leached nitrogen enters the water system in the form of small organic molecules, mitigating the negative damage caused by inorganic nitrogen.

## 5. Conclusions

In this study, natural superabsorbent polymers (SAPs) were prepared by polyglutamic acid, diatomite, and pullulan polysaccharide and combined with biochar to make co-coated slow-release urea suitable for rice systems. Grafting copolymerization with diatomite and the formation of a semi-interpenetrating polymer network increased the water absorbency of SAPs by 11–20%, with the highest absorbance of  $652 \pm 38.2$  and  $56.2 \pm 4.7 \text{ g g}^{-1}$  in deionized water and 0.9% NaCl solutions. The modified double-layer co-coated urea had excellent slow-release properties, which significantly ( $p < 0.05$ ) increased rice grain yield ( $9.88 \pm 3.6\%$ ), plant N uptake ( $17.2 \pm 4.8\%$ ), and reduced fertilizer N losses ( $30.4 \pm 7.2\%$ ) over the entire life period. The modified SAPs could enable the nutrient release curve to better match the rice dynamic nutrient requirements. Therefore, natural SAPs prepared on the basis of polyglutamic acid will be a strong competitor to conventional synthetic SAPs to relieve the widespread nitrogen loss in rice systems.

**Author Contributions:** Conceptualization, L.C. and F.G.; methodology, L.W., L.C., and F.G.; software, L.W.; validation, L.C.; formal analysis, L.W.; investigation, L.C.; resources, L.C.; data curation, L.W. and F.G.; writing—original draft preparation, L.W.; writing—review and editing, L.C. and F.W.; visualization, L.W.; supervision, F.G.; project administration, L.C. and Y.W.; funding acquisition, L.C. and Y.W. All authors have read and agreed to the published version of the manuscript.

**Funding:** This research was funded by the Natural Science Foundation of the Anhui Higher Education Institutions of China, grant number 2022AH052438.

**Institutional Review Board Statement:** Not applicable.

**Data Availability Statement:** Data will be made available on request.

**Acknowledgments:** We acknowledge the support of the Natural Science Foundation of the Anhui Higher Education Institutions of China (grant numbers: 2022AH052438) for this study. Thanks to Yanping Wang and Fuyong Wu of Northwest A&F University for providing the experimental sites.

**Conflicts of Interest:** The authors declare no conflicts of interest.

## References

1. Cai, S.; Zhao, X.; Pittelkow, C.M.; Fan, M.; Zhang, X.; Yan, X. Optimal nitrogen rate strategy for sustainable rice production in China. *Nature* **2023**, *615*, 73–79. [[CrossRef](#)]
2. Cui, Z.; Zhang, H.; Chen, X.; Zhang, C.; Ma, W.; Huang, C.; Zhang, W.; Mi, G.; Miao, Y.; Li, X.; et al. Pursuing sustainable productivity with millions of smallholder farmers. *Nature* **2018**, *555*, 363–366. [[CrossRef](#)]
3. Yang, X.; Xiong, J.; Du, T.; Ju, X.; Gan, Y.; Li, S.; Xia, L.; Shen, Y.; Pacenka, S.; Steenhuis, T.S.; et al. Diversifying crop rotation increases food production, reduces net greenhouse gas emissions and improves soil health. *Nat. Commun.* **2024**, *15*, 198. [[CrossRef](#)]
4. Raza, S.; Miao, N.; Wang, P.; Ju, X.; Chen, Z.; Zhou, J.; Kuzyakov, Y. Dramatic loss of inorganic carbon by nitrogen-induced soil acidification in Chinese croplands. *Glob. Chang. Biol.* **2020**, *26*, 3738–3751. [[CrossRef](#)]
5. Xin, Y.; Wenhai, M.; Shaofu, W.; Lianghuan, W.; Jianqiu, C. Rice responses to single application of coated urea on yield, dry matter accumulation, and nitrogen uptake in Southern China. *J. Plant Nutr.* **2017**, *40*, 2181–2191. [[CrossRef](#)]
6. Shi, W.; Zhang, Q.; Xie, R.; Sheng, K.; Tan, J.; Wang, Y. Blending loss-control and normal urea maximizes nitrogen utilization of summer maize by mitigating ammonia volatilization and nitrate leaching. *Plant Soil.* **2023**, *490*, 125–141. [[CrossRef](#)]
7. Ning, T.Y.; Shao, G.Q.; Li, Z.J.; Han, H.F.; Hu, H.G.; Wang, Y.; Tian, S.Z.; Chi, S.Y. Effects of urea types and irrigation on crop uptake, soil residual, and loss of nitrogen in maize field on the North China Plain. *Plant Soil. Environ.* **2012**, *58*, 1–8. [[CrossRef](#)]
8. Hu, H.; Ning, T.; Li, Z.; Han, H.; Zhang, Z.; Qin, S.; Zheng, Y. Coupling effects of urea types and subsoiling on nitrogen–water use and yield of different varieties of maize in northern China. *Field Crop. Res.* **2013**, *142*, 85–94. [[CrossRef](#)]

9. Li, P.; Lu, J.; Wang, Y.; Wang, S.; Hussain, S.; Ren, T.; Cong, R.; Li, X. Nitrogen losses, use efficiency, and productivity of early rice under controlled-release urea. *Agric. Ecosyst. Environ.* **2018**, *251*, 78–87. [[CrossRef](#)]
10. Han, X.; Chen, S.; Hu, X. Controlled-release fertilizer encapsulated by starch/polyvinyl alcohol coating. *Desalination* **2009**, *240*, 21–26. [[CrossRef](#)]
11. Azeem, B.; KuShaari, K.; Man, Z.B.; Basit, A.; Thanh, T.H. Review on materials & methods to produce controlled release coated urea fertilizer. *J. Control. Release* **2014**, *181*, 11–21. [[CrossRef](#)] [[PubMed](#)]
12. Ma, X.; Chen, J.; Yang, Y.; Su, X.; Zhang, S.; Gao, B.; Li, Y.C. Siloxane and polyether dual modification improves hydrophobicity and interpenetrating polymer network of bio-polymer for coated fertilizers with enhanced slow release characteristics. *Chem. Eng. J.* **2018**, *350*, 1125–1134. [[CrossRef](#)]
13. Guo, J.; Shi, W.; Wang, P.; Hao, Q.; Li, J. Performance characterization of  $\gamma$ -poly (glutamic acid) super absorbent polymer and its effect on soil water availability. *Arch. Agron. Soil Sci.* **2021**, *68*, 1145–1158. [[CrossRef](#)]
14. An, X.; Wu, Z.; Qin, H.; Liu, X.; He, Y.; Xu, X.; Li, T.; Yu, B. Integrated co-pyrolysis and coating for the synthesis of a new coated biochar-based fertilizer with enhanced slow-release performance. *J. Clean. Prod.* **2021**, *283*, 124642. [[CrossRef](#)]
15. Dong, Z.; Qu, N.; Jiang, Q.; Han, Z.; Sun, L.; Zhang, T.; Liang, D.; Shi, Y.; Cheng, Z. Preparation and properties of multifunctional eco-friendly slow-release urea fertilizer encapsulated by diatomite filter aid waste-based superabsorbent. *Prog. Org. Coat.* **2023**, *183*, 107747. [[CrossRef](#)]
16. Guo, J.Z.; Zhang, K.P.; Zhang, J.J.; Li, S.; Zhang, Y.K. Effects of Poly- $\Gamma$ -Glutamic Acid Super Absorbent Polymer on Soil Microenvironment and Growth of Winter Wheat. *Appl. Ecol. Environ. Res.* **2023**, *21*, 2457–2475. [[CrossRef](#)]
17. Zohuriaan-Mehr, M.J.; Kabiri, K. Superabsorbent polymer materials a review. *Iran. Polym. J.* **2008**, *17*, 451–477. [[CrossRef](#)]
18. Guo, J.; Shi, W.; Wen, L.; Shi, X.; Li, J. Effects of a super-absorbent polymer derived from poly- $\gamma$ -glutamic acid on water infiltration, field water capacity, soil evaporation, and soil water-stable aggregates. *Arch. Agron. Soil Sci.* **2019**, *66*, 1627–1638. [[CrossRef](#)]
19. Guo, J.; Zhang, J.; Zhang, K.; Li, S.; Zhang, Y. Effect of  $\gamma$ -PGA and  $\gamma$ -PGA SAP on soil microenvironment and the yield of winter wheat. *PLoS ONE* **2023**, *18*, e0288299. [[CrossRef](#)] [[PubMed](#)]
20. Bai, Y.; Chen, S.; Fan, L.; Yang, M.; Zou, H.; Zhang, Y. Preparation and properties of nano-SiO<sub>2</sub>–polyvinyl alcohol– $\gamma$ -polyglutamic acid composite film materials. *J. Plant Nutr. Fertil.* **2019**, *25*, 2044–2052. [[CrossRef](#)]
21. Lin, W.C.; Yu, D.G.; Yang, M.C. Blood compatibility of novel poly(gamma-glutamic acid)/polyvinyl alcohol hydrogels. *Colloid Surf. B* **2006**, *47*, 43–49. [[CrossRef](#)] [[PubMed](#)]
22. Lee, Y.G.; Kang, H.S.; Kim, M.S.; Son, T.I. Thermally crosslinked anionic hydrogels composed of poly(vinyl alcohol) and poly( $\gamma$ -glutamic acid): Preparation, characterization, and drug permeation behavior. *J. Appl. Polym. Sci.* **2008**, *109*, 3768–3775. [[CrossRef](#)]
23. Qiu, K.; Netravali, A.N. Bacterial cellulose-based membrane-like biodegradable composites using cross-linked and noncross-linked polyvinyl alcohol. *J. Mater. Sci.* **2012**, *47*, 6066–6075. [[CrossRef](#)]
24. Wu, Y.; Wang, S.; Zhou, D.; Zhang, Y.; Wang, X.; Yang, R. Biodegradable polyvinyl alcohol nanocomposites made from rice straw fibrils: Mechanical and thermal properties. *J. Compos. Mater.* **2012**, *47*, 1449–1459. [[CrossRef](#)]
25. Zhang, H.; Xing, L.; Liang, H.; Liu, S.; Ding, W.; Zhang, J.; Xu, C. Preparation and characterization of biochar-based slow-release nitrogen fertilizer and its effect on maize growth. *Ind. Crops Prod.* **2023**, *203*, 117227. [[CrossRef](#)]
26. Yang, Y.; Liang, Z.; Zhang, R.; Zhou, S.; Yang, H.; Chen, Y.; Zhang, J.; Yin, H.; Yu, D. Research Advances in Superabsorbent Polymers. *Polymers* **2024**, *16*, 501. [[CrossRef](#)]
27. Omidian, H.; Akhzarmehr, A.; Chowdhury, S.D. Advancements in Cellulose-Based Superabsorbent Hydrogels: Sustainable Solutions across Industries. *Gels* **2024**, *10*, 174. [[CrossRef](#)] [[PubMed](#)]
28. Chen, X.; Chen, S.; Sun, M.; Yu, Z. High yield of poly-gamma-glutamic acid from *Bacillus subtilis* by solid-state fermentation using swine manure as the basis of a solid substrate. *Bioresour. Technol.* **2005**, *96*, 1872–1879. [[CrossRef](#)]
29. Rampichová, M.; Kostáková, E.; Filová, E.; Prosecká, E.; Plencner, M.; Ocheretná, L.; Lytvynets, A.; Lukás, D.; Amler, E. Non-Woven PGA/PVA Fibrous Mesh as an Appropriate Scaffold for Chondrocyte Proliferation. *Physiol. Res.* **2010**, *59*, 773–781. [[CrossRef](#)]
30. Souri, M.K.; Hatamian, M. Aminochelates in plant nutrition: A review. *J. Plant Nutr.* **2018**, *42*, 67–78. [[CrossRef](#)]
31. Ohtake, N.; Nishiwaki, T.; Mizukoshi, K.; Minagawa, R.; Takahashi, Y.; Chinushi, T.; Ohyama, T. Amino acid composition in xylem sap of soybean related to the evaluation of N<sub>2</sub> fixation by the relative ureide method. *Soil Sci. Plant Nutr.* **1995**, *41*, 95–102. [[CrossRef](#)]
32. Chen, L.; Fei, L.; Wang, Z.; Salahou, M.K.; Liu, L.; Zhong, Y.; Dai, Z. The effects of ploy ( $\gamma$ -glutamic acid) on spinach productivity and nitrogen use efficiency in North-West China. *Plant Soil Environ.* **2018**, *64*, 517–522. [[CrossRef](#)]
33. Xu, Z.; Wan, C.; Xu, X.; Feng, X.; Xu, H. Effect of poly ( $\gamma$ -glutamic acid) on wheat productivity, nitrogen use efficiency and soil microbes. *J. Plant Nutr. Soil Sci.* **2013**, *13*, 744–755. [[CrossRef](#)]
34. Kenawy, E.-R.; Azaam, M.M.; El-nshar, E.M. Sodium alginate-g-poly(acrylic acid-co-2-hydroxyethyl methacrylate)/montmorillonite superabsorbent composite: Preparation, swelling investigation and its application as a slow-release fertilizer. *Arab. J. Chem.* **2019**, *12*, 847–856. [[CrossRef](#)]
35. Peng, N.; Wang, Y.; Ye, Q.; Liang, L.; An, Y.; Li, Q.; Chang, C. Biocompatible cellulose-based superabsorbent hydrogels with antimicrobial activity. *Carbohydr. Polym.* **2016**, *137*, 59–64. [[CrossRef](#)] [[PubMed](#)]

36. Dhand, A.P.; Galarraga, J.H.; Burdick, J.A. Enhancing Biopolymer Hydrogel Functionality through Interpenetrating Networks. *Trends Biotechnol.* **2021**, *39*, 519–538. [[CrossRef](#)]
37. Dragan, E.S. Design and applications of interpenetrating polymer network hydrogels. A review. *Chem. Eng. J.* **2014**, *243*, 572–590. [[CrossRef](#)]
38. Ghazali, S.; Jamar, S.; Noordin, N.; Tan, K.M. Properties of Controlled-Release-Water-Retention Fertilizer Coated with Carbonaceous-g-Poly (acrylic acid-co-acrylamide) Superabsorbent Polymer. *Int. J. Chem. Eng. Appl.* **2017**, *8*, 141–147. [[CrossRef](#)]
39. Ahmadian, M.; Jaymand, M. Interpenetrating polymer network hydrogels for removal of synthetic dyes: A comprehensive review. *Coordin. Chem. Rev.* **2023**, *486*, 215152. [[CrossRef](#)]
40. Dong, D.; Li, J.; Ying, S.; Wu, J.; Han, X.; Teng, Y.; Zhou, M.; Ren, Y.; Jiang, P. Mitigation of methane emission in a rice paddy field amended with biochar-based slow-release fertilizer. *Sci. Total Environ.* **2021**, *792*, 148460. [[CrossRef](#)]
41. Wang, C.; Luo, D.; Zhang, X.; Huang, R.; Cao, Y.; Liu, G.; Zhang, Y.; Wang, H. Biochar-based slow-release of fertilizers for sustainable agriculture: A mini review. *Environ. Sci. Ecotechnol.* **2022**, *10*, 100167. [[CrossRef](#)]
42. Luo, D.; Wang, L.; Nan, H.; Cao, Y.; Wang, H.; Kumar, T.V.; Wang, C. Phosphorus adsorption by functionalized biochar: A review. *Environ. Chem. Lett.* **2022**, *21*, 497–524. [[CrossRef](#)]
43. Ding, Y.; Liu, Y.; Liu, S.; Li, Z.; Tan, X.; Huang, X.; Zeng, G.; Zhou, L.; Zheng, B. Biochar to improve soil fertility. A review. *Agron. Sustain. Dev.* **2016**, *36*, 36. [[CrossRef](#)]
44. Cheng, S.; Zeng, W.; Liu, X.; Zhao, J.; Qiu, X.; Lei, Z. Anti-evaporation Performance of Water in Soil of Superabsorbent Resin with Fast Water Absorption Rate. *Water Air Soil Pollut.* **2020**, *231*, 1–15. [[CrossRef](#)]
45. Arafa, E.; Sabaa, M.; Mohamed, R.; Elzanaty, A.; Abdel-Gawad, O. Preparation of biodegradable sodium alginate/carboxymethylchitosan hydrogels for the slow-release of urea fertilizer and their antimicrobial activity. *React. Funct. Polym.* **2022**, *174*, 105243. [[CrossRef](#)]
46. Jensen, E.S.; Carlsson, G.; Hauggaard-Nielsen, H. Intercropping of grain legumes and cereals improves the use of soil N resources and reduces the requirement for synthetic fertilizer N: A global-scale analysis. *Agron. Sustain. Dev.* **2020**, *40*, 5. [[CrossRef](#)]
47. Craine, J.M.; Brookshire, E.N.J.; Cramer, M.D.; Hasselquist, N.J.; Koba, K.; Marin-Spiotta, E.; Wang, L. Ecological interpretations of nitrogen isotope ratios of terrestrial plants and soils. *Plant Soil* **2015**, *396*, 1–26. [[CrossRef](#)]
48. Wang, H.; Hu, R.-G.; Lin, S.; Gao, H.-J.; Xu, M.-G.; Zhang, W.-J.; Wu, L. Effects of Long-term Application of Organic and Chemical Fertilizers on N<sub>2</sub>O Emissions from Black Soils. *Environ. Sci.* **2024**, *46*, 202401053. [[CrossRef](#)]
49. Bradford, M.A.; Strickland, M.S.; DeVore, J.L.; Maerz, J.C. Root carbon flow from an invasive plant to belowground foodwebs. *Plant Soil* **2012**, *359*, 233–244. [[CrossRef](#)]
50. De Troyer, I.; Amery, F.; Van Moorleghe, C.; Smolders, E.; Merckx, R. Tracing the source and fate of dissolved organic matter in soil after incorporation of a <sup>13</sup>C labelled residue: A batch incubation study. *Soil Biol. Biochem.* **2011**, *43*, 513–519. [[CrossRef](#)]
51. Kou, X.; Morrien, E.; Tian, Y.; Zhang, X.; Lu, C.; Xie, H.; Liang, W.; Li, Q.; Liang, C. Exogenous carbon turnover within the soil food web strengthens soil carbon sequestration through microbial necromass accumulation. *Glob. Chang. Biol.* **2023**, *29*, 4069–4080. [[CrossRef](#)]
52. Bland, A.; Lerch, T.Z.; Chevallier, T.; Nunan, N.; Chenu, C.; Brauman, A. Dynamics of bacterial communities in relation to soil aggregate formation during the decomposition of <sup>13</sup>C-labelled rice straw. *Appl. Soil Ecol.* **2012**, *53*, 1–9. [[CrossRef](#)]
53. Denk, T.R.A.; Mohn, J.; Decock, C.; Lewicka-Szczebak, D.; Harris, E.; Butterbach-Bahl, K.; Kiese, R.; Wolf, B. The nitrogen cycle: A review of isotope effects and isotope modeling approaches. *Soil Biol. Biochem.* **2017**, *105*, 121–137. [[CrossRef](#)]
54. Cotrufo, M.F.; Ranalli, M.G.; Haddix, M.L.; Six, J.; Lugato, E. Soil carbon storage informed by particulate and mineral-associated organic matter. *Nat. Geosci.* **2019**, *12*, 989–994. [[CrossRef](#)]
55. Gurmesa, G.A.; Wang, A.; Li, S.; Peng, S.; de Vries, W.; Gundersen, P.; Ciais, P.; Phillips, O.L.; Hobbie, E.A.; Zhu, W.; et al. Retention of deposited ammonium and nitrate and its impact on the global forest carbon sink. *Nat. Commun.* **2022**, *13*, 880. [[CrossRef](#)]
56. Ma, Q.; Wen, Y.; Wang, D.; Sun, X.; Hill, P.W.; Macdonald, A.; Chadwick, D.R.; Wu, L.; Jones, D.L. Farmyard manure applications stimulate soil carbon and nitrogen cycling by boosting microbial biomass rather than changing its community composition. *Soil Biol. Biochem.* **2020**, *144*, 107760. [[CrossRef](#)]
57. Tao, J.; Raza, S.; Zhao, M.; Cui, J.; Wang, P.; Sui, Y.; Zamanian, K.; Kuzyakov, Y.; Xu, M.; Chen, Z.; et al. Vulnerability and driving factors of soil inorganic carbon stocks in Chinese croplands. *Sci. Total Environ.* **2022**, *825*, 154087. [[CrossRef](#)] [[PubMed](#)]
58. Mirbolook, A.; Sadaghiani, M.R.; Keshavarz, P.; Alikhani, M. New Slow-Release Urea Fertilizer Fortified with Zinc for Improving Zinc Availability and Nitrogen Use Efficiency in Maize. *ACS Omega* **2023**, *8*, 45715–45728. [[CrossRef](#)] [[PubMed](#)]
59. Mukerabigwi, J.F.; Wang, Q.; Ma, X.; Liu, M.; Lei, S.; Wei, H.; Huang, X.; Cao, Y. Urea fertilizer coated with biodegradable polymers and diatomite for slow release and water retention. *J. Coat. Technol. Res.* **2015**, *12*, 1085–1094. [[CrossRef](#)]
60. Li, X.; Luo, J.; Li, J.; Gao, Q. Effects of diatomite inorganic fillers on the properties of a melamine-urea-formaldehyde resin. *J. Appl. Polym. Sci.* **2016**, *133*, 44095. [[CrossRef](#)]
61. Sun, Y.; Wang, R.; Liu, X.; Dai, E.; Li, B.; Fang, S.; Li, D. Synthesis and Performances of Phase Change Microcapsules with a Polymer/Diatomite Hybrid Shell for Thermal Energy Storage. *Polymers* **2018**, *10*, 601. [[CrossRef](#)] [[PubMed](#)]
62. Xiu, K.; Wen, J.; Porteous, N.; Sun, Y. Controlling bacterial fouling with polyurethane/N-halamine semi-interpenetrating polymer networks. *J. Bioact. Compat. Pol.* **2017**, *32*, 542–554. [[CrossRef](#)]
63. Frounchi, M.; Burford, R.P.; Chaplin, R.P. Interpenetrating polymer networks of poly(diethyleneglycol bis(allylcarbonate)) and poly(urethane acrylates). *Polymer* **1994**, *35*, 5073–5078. [[CrossRef](#)]

64. Wang, M.; Jiang, J.; Liang, S.; Sui, C.; Wu, S. Functional Semi-Interpenetrating Polymer Networks. *Macromol. Rapid Comm.* **2024**, *30*, e2400539. [[CrossRef](#)] [[PubMed](#)]
65. Rastogi, A.; Tripathi, D.K.; Yadav, S.; Chauhan, D.K.; Zivcak, M.; Ghorbanpour, M.; El-Sheery, N.I.; Brestic, M. Application of silicon nanoparticles in agriculture. *3 Biotech* **2019**, *9*, 90. [[CrossRef](#)]
66. Haynes, R.J. A contemporary overview of silicon availability in agricultural soils. *J. Plant Nutr. Soil Sci.* **2014**, *177*, 831–844. [[CrossRef](#)]
67. Mir, R.A.; Bhat, B.A.; Yousuf, H.; Islam, S.T.; Raza, A.; Rizvi, M.A.; Charagh, S.; Albaqami, M.; Sofi, P.A.; Zargar, S.M. Multidimensional Role of Silicon to Activate Resilient Plant Growth and to Mitigate Abiotic Stress. *Front. Plant Sci.* **2022**, *13*, 819658. [[CrossRef](#)]
68. Coskun, D.; Britto, D.T.; Huynh, W.Q.; Kronzucker, H.J. The Role of Silicon in Higher Plants under Salinity and Drought Stress. *Front. Plant Sci.* **2016**, *7*, 1072. [[CrossRef](#)]
69. Paleckiene, R.; Sviklas, A.; Šlinkšienė, R. Physicochemical properties of a microelement fertilizer with amino acids. *Russ. J. Appl. Chem.* **2007**, *80*, 352–357. [[CrossRef](#)]
70. Liu, Y.; Kong, S.; Li, Y.; Zeng, H. Novel technology for sewage sludge utilization: Preparation of amino acids chelated trace elements (AACTE) fertilizer. *J. Hazard. Mater.* **2009**, *171*, 1159–1167. [[CrossRef](#)]
71. Zou, J.; Huang, Y.; Qin, Y.; Liu, S.; Shen, Q.; Pan, G.; Lu, Y.; Liu, Q. Changes in fertilizer-induced direct N<sub>2</sub>O emissions from paddy fields during. *Glob. Chang. Biol.* **2009**, *15*, 229–242. [[CrossRef](#)]
72. Inamura, T.; Mukai, Y.; Maruyama, A.; Ikenaga, S.; Li, G.U.; Bu, X.; Xiang, Y.; Qin, D.; Amano, T. Effects of nitrogen mineralization on paddy rice yield under low nitrogen input conditions in irrigated rice-based multiple cropping with intensive cropping of vegetables in southwest China. *Plant Soil* **2009**, *315*, 195–209. [[CrossRef](#)]
73. Ma, Y.; Wu, J.; Fan, S.; Yu, S. Towards Less Agricultural Nitrogen Use in China: Perspective from a Multi-Crop and Multi-Region Partial Equilibrium Analysis. *Pol. J. Environ. Stud.* **2023**, *32*, 4713–4723. [[CrossRef](#)]
74. Kahrl, F.; Li, Y.; Su, Y.; Tennigkeit, T.; Wilkes, A.; Xu, J. Greenhouse gas emissions from nitrogen fertilizer use in China. *Environ. Sci. Policy* **2010**, *13*, 688–694. [[CrossRef](#)]
75. Bai, Z.; Xie, C.; Yu, J.; Bai, W.; Pei, S.; Li, Y.; Li, Z.; Zhang, F.; Fan, J.; Yin, F. Effects of irrigation and nitrogen levels on yield and water-nitrogen-radiation use efficiency of drip-fertigated cotton in south Xinjiang of China. *Field Crop. Res.* **2024**, *308*, 109280. [[CrossRef](#)]
76. Zamanian, K.; Zarebanadkouki, M.; Kuzyakov, Y. Nitrogen fertilization raises CO<sub>2</sub> efflux from inorganic carbon: A global assessment. *Glob. Chang. Biol.* **2018**, *24*, 2810–2817. [[CrossRef](#)]
77. Wu, L.; Chen, X.; Wei, W.; Liu, Y.; Wang, D.; Ni, B.J. A Critical Review on Nitrous Oxide Production by Ammonia-Oxidizing Archaea. *Environ. Sci. Technol.* **2020**, *54*, 9175–9190. [[CrossRef](#)] [[PubMed](#)]
78. Guo, F.; Wang, Y.; Zhu, H.; Zhang, C.; Sun, H.; Fang, Z.; Yang, J.; Zhang, L.; Mu, Y.; Man, Y.B.; et al. Crop productivity and soil inorganic carbon change mediated by enhanced rock weathering in farmland: A comparative field analysis of multi-agroclimatic regions in central China. *Agric. Syst.* **2023**, *210*, 103691. [[CrossRef](#)]
79. Lassaletta, L.; Billen, G.; Grizzetti, B.; Anglade, J.; Garnier, J. 50 year trends in nitrogen use efficiency of world cropping systems: The relationship between yield and nitrogen input to cropland. *Environ. Res. Lett.* **2014**, *9*, 105011. [[CrossRef](#)]
80. Guo, Y.; Chen, Y.; Searchinger, T.D.; Zhou, M.; Pan, D.; Yang, J.; Wu, L.; Cui, Z.; Zhang, W.; Zhang, F.; et al. Air quality, nitrogen use efficiency and food security in China are improved by cost-effective agricultural nitrogen management. *Nat. Food* **2020**, *1*, 648–658. [[CrossRef](#)]
81. Lu, J.; Hu, T.; Zhang, B.; Wang, L.; Yang, S.; Fan, J.; Yan, S.; Zhang, F. Nitrogen fertilizer management effects on soil nitrate leaching, grain yield and economic benefit of summer maize in Northwest China. *Agric. Water Manag.* **2021**, *247*, 106739. [[CrossRef](#)]

**Disclaimer/Publisher's Note:** The statements, opinions and data contained in all publications are solely those of the individual author(s) and contributor(s) and not of MDPI and/or the editor(s). MDPI and/or the editor(s) disclaim responsibility for any injury to people or property resulting from any ideas, methods, instructions or products referred to in the content.